Available online at www.sciencedirect.com
SCIENCE DIRECT
Journal of Power Sources 156 (2006) 598–603
JOURNAL OF POWER SOURCES
www.elsevier.com/locate/jpowsour

Short communication

Influence of magnetic properties on electrochemical activity of $LiNi_{0.5}Fe_{0.5}O_2$

D. Kalpana [a,*], R. Justin Joseyphus [b], C. Venkateswaran [b], A. Narayanasamy [b], M.V. Ananth [a]

[a] *Central Electrochemical Research Institute, Karaikudi, Tamilnadu 630 006, India*
[b] *Materials Science Centre, Department of Nuclear Physics, University of Madras, Guindy Campus, Chennai, Tamilnadu 600 025, India*

Received 3 March 2005; accepted 30 May 2005
Available online 18 August 2005

Abstract

$LiNi_{0.5}Fe_{0.5}O_2$ is prepared by a sol–gel method and the sample is heat-treated to various temperatures to characterize its physico-chemical properties. Calcination of the precursor at 673 K produces powders of tetragonal and hexagonal phases. Subsequent heat treatment at 873, 1073 and 1273 K results in a pure hexagonal phase. Vibrating sample magnetometer (VSM) studies show that the tetragonal phase is magnetically stronger than the hexogonal phase. Room-temperature Mössbauer studies reveal magnetic ordering for the tetragonal phase and the paramagnetic nature of the hexagonal phase. The hexagonal phase is magnetically ordered at 77 K. By comparing the value of the hyperfine field with the bulk magnetization value at 77 K obtained from VSM, it is concluded that the magnetic ordering cannot be ferromagnetic but should be antiferromagnetic.

PACS: 75.50 Ee; 76.80.+y

Keywords: $LiCo_{0.5}Fe_{0.5}O_2$; Mössbauer effect; Triangular antiferromagnetism; Lithium-ion battery; Magnetic properties

1. Introduction

Among the rechargeable battery systems, lithium-ion batteries offer higher specific energy, light weight and long cycle-life, all of which are essential to meet the requirements of portable electronic equipment [1]. The compound $LiNiO_2$ has been extensively investigated as a positive active material because of its comparatively low cost, large theoretical capacity (275 mAh g^{-1}) and environmental advantages over $LiCoO_2$ [2–4]. The discharge capacity of non-stoichiometric $LiNiO_2$ has been shown experimentally to be about 140–150 mAh g^{-1} [5].

$LiNiO_2$ has the rhombohedral structure with a trigonal symmetry *R*3*m* space group. It consists of the alternate layers of Li and Ni that occupy the octahedral sites of a cubic-closed-packed oxide lattice. This structure provides the basis for a triangular lattice at low temperatures and enables lithium-ions to intercalate and de-intercalate reversibly at high temperatures. The parameters of the unit cell are usually defined in terms of the hexagonal setting [6–8].

Lithiated transition metal oxides $LiMO_2$ (M = Ni, Co, Fe, Mn) have been synthesized using solid-state approaches that require prolonged heat treatment at high temperatures. These conditions may result in non-homogeneity, abnormal grain growth and poor control of stoichiometry [9–13]. It is difficult to synthesize stoichiometric $LiNiO_2$ because of loss of lithium from the host structure during high temperature calcination due to the high vapour pressure of lithium [14]. This leads to the formation of a non-stoichiometric $[Li_{1-x}Ni_x]_{3b}[Ni_{1-x}]_{3a}[O_2]_{6c}$ structure that, in turn, results in a low initial capacity of $LiNiO_2$ followed by capacity loss during cycling [15].

A method using excess lithium has been employed in a solid-state reaction to synthesize stoichiometric $LiNiO_2$

* Corresponding author. Tel.: +91 4565 227 550/551; fax: +91 4565 227 651.
E-mail address: kalpss@yahoo.com (D. Kalpana).

0378-7753/$ – see front matter © 2005 Elsevier B.V. All rights reserved.
doi:10.1016/j.jpowsour.2005.05.097

[16–18]. This method does, however, require the removal of the small quantities of unreacted lithium by a washing step with deionized water. A sol–gel method has frequently been utilized to synthesize stoichiometric lithium metal oxides [19,20]. Meanwhile, improvements in the cycle-life of $LiNiO_2$ electrodes have extensively been sought by the partial substitution of nickel by transition metals, M, to make $LiM_xNi_{1-x}O_2$ (M = Al, Co, Fe, etc.) [21]. It has been reported [22] that the substitution process stabilizes the crystal structure of the material during intercalation/de-intercalation of lithium ions, even at the overcharged state, and thereby improves $LiNiO_2$ cycleability.

In this study, a sol–gel process is used to synthesize $LiNiO_2$ with partial replacement of Ni by Fe to form $LiNi_{0.5}Fe_{0.5}O_2$. It is possible to obtain the phase-pure, ultra-fine, crystalline, single-phase compound by employing temperatures for a few hours using the sol–gel method. The optimum conditions for the preparation of $LiNi_{0.5}Fe_{0.5}O_2$ have been investigated. Although structural and morphological techniques have been attempted on $LiNiO_2$, there has been little investigation of the magnetic properties by means of Mössbauer spectroscopy. The latter technique is highly useful to study the local structure and magnetic properties of materials. In the present work, detailed phase evolution, morphology, magnetic properties and discharge characteristics have been examined for cathode materials subjected to various heat treatments.

2. Experimental

2.1. Material synthesis

The oxide $LiNi_{0.5}Fe_{0.5}O_2$ was prepared from lithium hydroxide monohydrate (Aldrich 99%), proper stoichiometric amounts of nickel hydroxide and α-Fe_2O_3 as starting materials. Methanol (500 ml) was used as a solvent to dissolve the stoichiometric amounts of lithium and nickel precursors. α-Fe_2O_3 was mixed with distilled water and was stirred well with the solvent. Dark-purple suspensions of colloidal particles were obtained. The gel was then dried to yield an organic polymer foam. Calcining the precursors in air at various temperatures for a period of a few hours resulted in fine powders.

2.2. Characterization

The structural and magnetic properties of the gel and oxide powders were characterized by several techniques. X-ray powder diffraction experiments were performed with a STOE (Germany) high-precision powder X-ray diffractometer using Cu Kα radiation. The magnetization and coercivity of the sample were measured with a vibrating sample magnetometer (EG & G—PARC, Model 4500) with a maximum applied field of 7 kOe. ^{57}Fe Mössbauer studies were carried out using a constant acceleration Mössbauer spectrometer (Weissel, Germany, Model No. MDU-1200) with a ^{57}Co (Rh) Mössbauer source maintained at room temperature. The Mössbauer spectrum was fitted with the least-squares method developed by Bent et al. [23,24]. The morphology of the heat-treated powders was examined with a JEOL-JSM-840A-scanning electron microscope.

2.3. Electrochemical cell assembly

The charge and discharge characteristics of the cathodes were investigated in a laboratory cell that was comprised of a cathode and a lithium metal anode that were separated by a separator. The cathode was comprised of 40 mg of active material ($LiNi_{0.5}Fe_{0.5}O_2$) and 8 mg of a mixture of acetylene black with PTFE (polytetrafluoroethylene) as a conducting binder. The mixture was pressed and dried at 120 °C for 12 h. The electrolyte solution was 1 M $LiClO_4$/EC + PC (EC = ethylene carbonate; PC = propylene carbonate). The cell fabrication was carried out in an argon-filled dry box. The cells were cycled in the range 4.2–3.0 V and the typical charge–discharge current was 0.4 mA cm^{-2}.

3. Results and discussion

3.1. X-ray analysis

X-ray diffraction (XRD) patterns for the materials annealed at various temperatures for 6 h in air are given in Fig. 1. The material annealed at 673 K has three phases: cubic, tetragonal and hexagonal. The various crystallographic phases and the lattice parameters of $LiNi_{0.5}Fe_{0.5}O_2$ annealed at different temperatures are listed in Table 1. The tetragonal

Table 1
Structural parameters of $LiNi_{0.5}Fe_{0.5}O_2$ sample annealed at various temperatures

Annealing temperature (K)	Lattice parameters (Å)		Cell volume (Å^3)	Crystal phase
	a	*c*		
673	7.94	24.98	1576.89	Tetragonal
673	14.35	2.87	513.74	Hexagonal
673	8.35	–	582.25	Cubic
873	2.943	14.400	105.75	Hexagonal
1073	2.938	14.411	107.73	Hexagonal
1273	2.937	14.436	107.86	Hexagonal

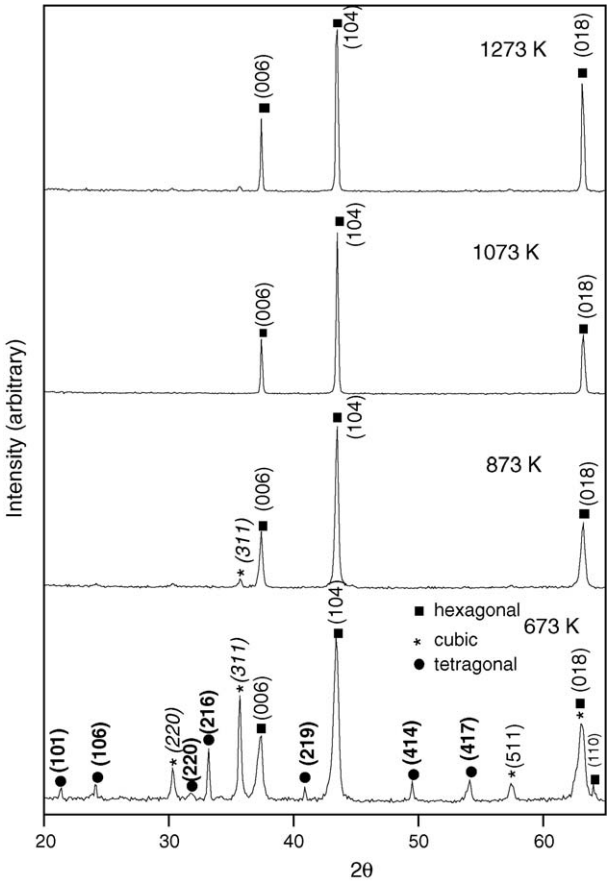

Fig. 1. X-ray powder diffraction pattern for $LiNi_{0.5}Fe_{0.5}O_2$ annealed at various temperatures.

phase disappears at 873 K and the pure hexagonal phase is formed at 1073 K. There is only a very small volume fraction of the cubic phase on annealing at 873 K, and this completely disappears on annealing at 1073 K. The cell volume is 105.75 Å^3 for the sample annealed at 873 K and increases to 107.8 Å^3 for the sample annealed at 1273 K due to texture effects.

3.2. Analysis with a vibrating sample magnetometer (VSM)

Magnetization data measured at room temperature and at 77 K for samples annealed at various temperatures between 673 and 1273 K are shown in Fig. 2. The specific magnetization (13.36 emu g^{-1}) obtained from the VSM experiments

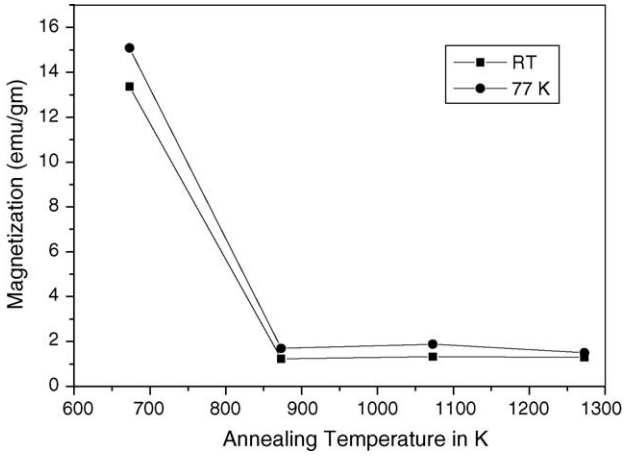

Fig. 2. Magnetization at RT and 77 K for $LiNi_{0.5}Fe_{0.5}O_2$ annealed at various temperatures. Solid lines are included as guides to the eyes.

is high for the sample annealed at 673 K, which has three phases, i.e., cubic hexagonal and tetragonal, as seen from XRD (Table 1), but is low for samples annealed at high temperatures that have a single hexagonal phase. The decrease in coercivity from 177.3 Oe for the sample at 673 K to 122.1 Oe (sample annealed at 1273 K) may be due to a reduction in strain by annealing at higher temperatures, as shown in Table 2. The magnetization is slightly higher at 77 K for all the samples annealed at various temperatures compared with that at room temperature (RT).

3.3. Mössbauer analysis

Room-temperature Mössbauer spectra of samples annealed at various temperatures are recorded in Fig. 3. The Mössbauer spectrum of the sample annealed at 673 K was fitted with one sextet and two doublets. The sextet arises from ^{57}Fe sites of the tetragonal phase with internal magnetic fields of 472 kOe at room temperature (Table 3). The two doublets arise from Fe in cubic and hexagonal phases. The relative intensities of the various spectral components of the Mössbauer spectrum are given in Table 3 and are in fairly good agreement with the relative intensities of the XRD peaks of the three phases.

The Mössbauer spectrum of the sample annealed at 873 K consists of only two doublets, i.e., the sextet is not present. The two doublets have been assigned to cubic and hexagonal phases. This shows that only the tetragonal phase is magnetically ordered at RT. Since the relative intensity of the cubic

Table 2
RT and 77 K magnetic parameters measured for sample annealed at various temperatures

Annealing temperature (K)	M_s (emu g^{-1})		H_c (Oe)		M_r/M_s	
	RT	77 K	RT	77 K	RT	77 K
673	13.36	15.08	177.3	287.2	0.27	0.31
873	1.23	1.69	155.0	190.0	0.13	0.12
1073	1.32	1.88	132.2	169.8	0.16	0.14
1273	1.30	1.50	122.1	130.9	0.15	0.14

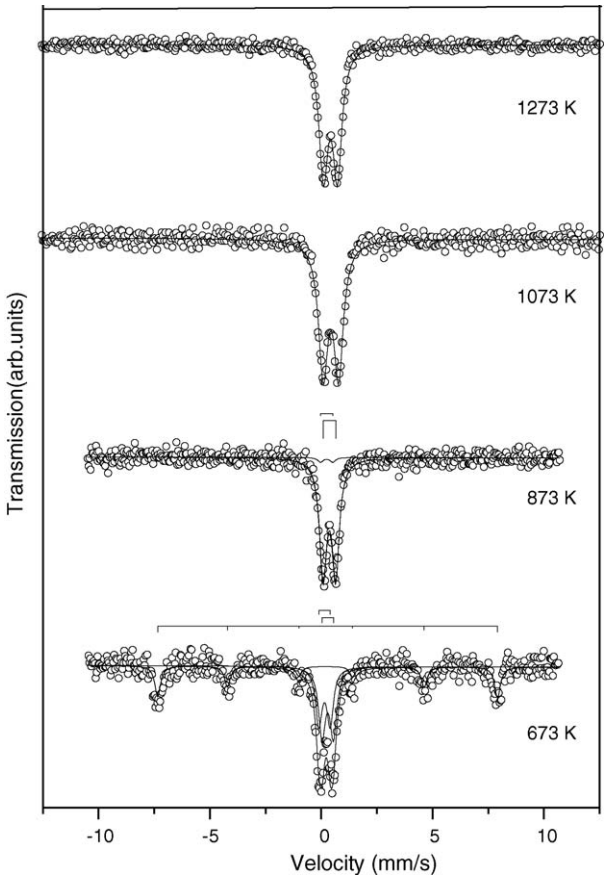

Fig. 3. Room-temperature Mössbauer spectra for samples annealed at various temperatures.

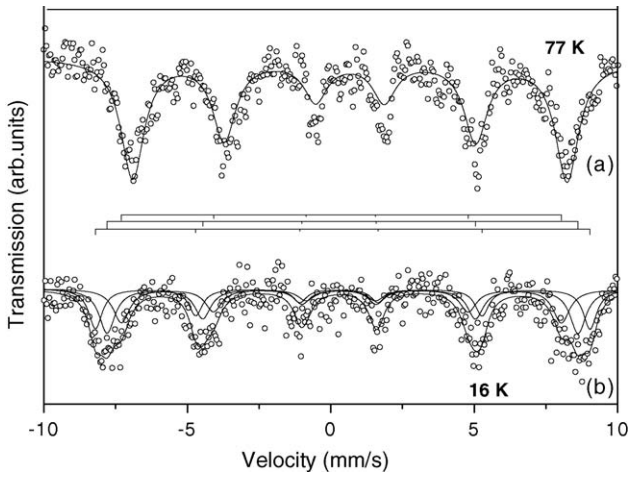

Fig. 4. Mössbauer spectrum of $LiNi_{0.5}Fe_{0.5}O_2$ sample measured at (a) 16 K for sample annealed at 673 K and (b) 77 K for sample annealed at 1073 K.

phase is only 3%, the XRD pattern does not show the presence of the cubic phase. On further annealing at 1073 and 1273 K, the sample gives rise to only a single quadrupole split doublet, which is assigned to the hexagonal phase in conformity with XRD data.

The information collated in Table 3 reveals that the decrease in quadrupole split value from 0.55 ± 0.01 mm s^{-1} (1073 K annealed) to 0.50 mm s^{-1} (1273 K annealed) for the hexagonal phase may be due to lattice ordering and lattice expansion, as revealed by XRD measurements. The isomer shift of 0.46 ± 0.01 mm s^{-1} shows that iron is in the ferric state.

In order to investigate whether the cubic and hexagonal phases are magnetic or non-magnetic, the Mössbauer spectrum of the 673 K-annealed sample was recorded at 16 K. The spectrum is shown in Fig. 4 and fitted with three sextets, i.e., one from each of the three crystallographic phases. No paramagnetic component is present at this temperature and this clearly indicates that both the hexagonal and the cubic phases are magnetic only and have very low ordering temperatures. In order to confirm this result, the Mössbauer spectrum was recorded at 77 K for the sample annealed at 1073 K. This spectrum, shown in Fig. 4, consists of a sextet and hence it is further confirmed that the hexagonal phase is magnetic with an ordering temperature above 77 K. The fitted Mössbauer parameters are presented in Table 4. The hyperfine magnetic field of the hexagonal phase at 77 K is 510 kOe, whereas the magnetization at this temperature is only 1.88 emu g^{-1} as reported in Table 2. This suggests that the hexagonal phase cannot be ferromagnetic and should be only an antiferromagnet. The ferromagnetic ordering

Table 3
RT Mössbauer parameters of $LiNi_{0.5}Fe_{0.5}O_2$ sample annealed at various temperatures

Annealing temperature (K)	Hyperfine magnetic field (kOe) ± 1.0	Chemical shift (mm s^{-1}) ± 0.01	Quadrupole splitting (mm s^{-1}) ± 0.01	Line width (mm s^{-1}) ± 0.01	Relative intensity (%)
673	472, 0.0, 0.0	0.35, 0.40, 0.25	0.08, 0.51, 0.51	0.31, 0.37, 0.35,	30, 39, 31
873	0.0, 0.0	0.49, 0.36	0.58, 0.57	0.40, 0.30	97, 3
1073	0.0	0.46	0.55	0.41	100
1273	0.0	0.44	0.50	0.39	100

Table 4
Mössbauer parameters of $LiNi_{0.5}Fe_{0.5}O_2$ sample measured at 77 K for sample annealed at 1073 K and at 16 K for sample annealed at 673 K

Temperature (K)	Hyperfine magnetic field (kOe) ± 2	Chemical shift (mm s^{-1}) ± 0.01	Quadrupole shift (mm s^{-1}) ± 0.01	Line width (mm s^{-1}) ± 0.01	Relative intensity (%)
77	510	0.48	0.11	1.11	100
16	534, 508, 475	0.46, 0.46, 0.47	0.13, 0.12, 0.02	0.57, 0.67, 0.70	30, 39, 31

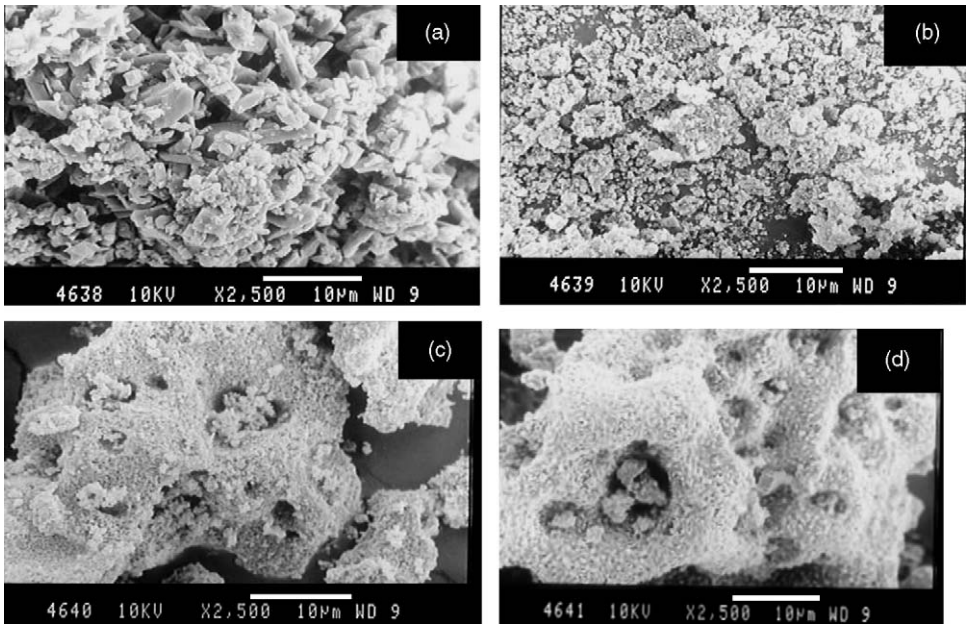

Fig. 5. SEM photographs of $LiNi_{0.5}Fe_{0.5}O_2$ samples: (a) as-prepared; (b) annealed at 673 K; (c) 600 K and (d) 800 K.

should have resulted in a larger value of the magnetization at 77 K.

3.4. Scanning electron microscopy (SEM) analysis

The textural stability of the positive electrode material is particularly well emphasized by a comparative SEM study performed on these materials. At a higher magnification, it is possible to distinguish the $LiNi_{0.5}Fe_{0.5}O_2$ crystallites that constitute the agglomerates.

A series of electron micrographs (Fig. 5) reveal the morphological changes that occur during calcination of the precursor. The as-prepared sample appears smooth and featureless (Fig. 5(a)) On heating to 673 K, clusters of particulates are seen (Fig. 5(b)). Electron micrographs of powders annealed at 873 and 1073 K for 6 h in air are shown in Fig. 5(c) and Fig. 6(d), respectively. The surface of the powders annealed at 1073 K contains mono-dispersed cuboidal fine particulates. The similarities between the two micrographs (1073 and 1273 K) show the textural stability of this material. These observations, together with XRD analysis, show clearly that the material has a single phase.

3.5. Discharge characteristics

The specific capacity and cyclability of the samples were determined by cycling the test cell at a constant current density of 0.4 mA cm^{-2} between 4.3 and 3.0 V. All the samples display excellent cycleability except for the sample annealed at 673 K and the as-prepared one, which has an impurity phase.

As shown in Fig. 6, the sample annealed at 673 K has a relatively small initial capacity and poor rechargeability. This

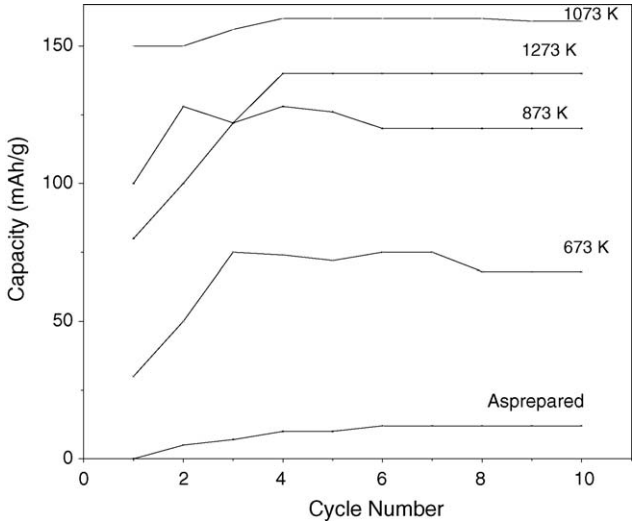

Fig. 6. Discharge characteristics of $LiNi_{0.5}Fe_{0.5}O_2$ annealed at various temperatures.

indicates that the sample does not have sufficient crystallinity and also that it has mixed phases. This is also consistent with XRD analysis, where the sample annealed at 673 K was found to consist of hexagonal, cubic and tetragonal phases. The poor electrochemical properties of the $LiNi_{0.5}Fe_{0.5}O_2$ cathode annealed at 873 K may be due to its two-phase (hexagonal and cubic) nature. The discharge capacity increases as the annealing temperature is raised from 873 to 1073 K, but then decreases on annealing at 1273 K. It has been reported that the smaller the surface area, the smaller is the initial discharge capacity and also most of the lithium intercalation/deintercalation process takes place at the surface rather than at the core of the grains [25].

For each sample, the electrochemical activity shows that the cell is activated only after the 5th cycle. The discharge capacity is low for the sample annealed at 673 K that has three phases, of which the tetragonal phase is magnetic at RT. The discharge capacity gradually increases on annealing at 873 K and above, which gives a paramagnetic hexagonal phase. It is observed that a sample with mixed phases and with one of them ferrimagnetically ordered is not suitable for electrochemical activity.

On the other hand the paramagnetic sample with a single crystallographic phase gave a maximum capacity of 160 mAh g^{-1}. The small decrease in the value of the discharge capacity of the 1273 K annealed sample compared with that of the 1073 K annealed sample may be due to changes in the microstructure produced by annealing at high temperatures. There is a remarkable increase in the discharge capacity for the sample annealed at 1073 K as it has a single hexagonal phase. Rechargeability is improved as the annealing temperature increases. This is due to the transition from multi phase to a single phase. It is concluded that the sample annealed at 1073 K has good structural and electrochemical properties. The initial coulombic efficiency is about 73%.

4. Conclusions

$LiNi_{0.5}Fe_{0.5}O_2$ has been prepared by a sol–gel method, samples have been heat-treated to various temperatures and their physico-chemical properties characterized. Calcination of the precursors at 673 K for 6 h produces powders that contain tetragonal and hexagonal phases. Subsequent heat treatment at 873, 1073 and 1273 K results in a pure hexagonal phase. The tetragonal phase is magnetically stronger than the hexagonal phase. Room-temperature Mössbauer studies reveal the magnetic ordering of the tetragonal phase and the paramagnetic nature of the hexagonal phase, which is magnetically ordered at 77 K. By analyzing the bulk magnetization with the value of hyperfine field, it is concluded that magnetic ordering cannot be ferromagnetic and should be only antiferromagnetic.

References

[1] J.M. Tarascon, M. Armand, Nature 414 (2000) 359.
[2] C. Delmas, Mater. Sci. Eng. B 3 (1989) 97.
[3] A.F. Wells, Structural Inorganic Chemistry, fifth ed., Oxford Science, London, 1991, p. 77.
[4] J.N. Feimers, W. Li, E. Rossen, Daha F. J.A, in: G.A. Nazri, J.M. Rarascon, M. Armand (Eds.), MRS Symposium Proceedings, vol. 293, MRS, Pittsburgh, 1993, p. 3.
[5] T. Ohzuku, H. Komon, M. Nagayama, K. Sawai, T. Hirai, Chem. Express. 6 (1991) 161.
[6] Z. Li, C. Wang, X. Ma, L. Yuan, J. Sun, Mater. Chem. Phys. 91 (2005) 36.
[7] A.G. Ritchie, J. Power Sources 136 (2004) 285.
[8] B.J. Hwang, R. Santhanam, C.H. Chen, J. Power Sources 114 (2003) 244.
[9] M. Tsuda, H. Arai, Masaya Takahashi, Hideaki Ohtsuka, Yoji Sakurai, Koji Sumitomo, Hiroyuki Kageshima, J. Power Sources 144 (2003) 183.
[10] Y. Kida, Katsunori Yanagida, Atsushi Yanai, Atsuhiro Funahashi, Toshiyuki Nohma, Ikuo Yonezu, J. Power Sources 142 (2005) 323.
[11] Chung-Cheih Chang, N. Scarr, P.N. Kumta, Solid State Ionics 112 (1998) 329.
[12] Z.S. Peng, C.R. Wan, C.Y. Jiang, J. Power Sources 72 (1998) 215.
[13] Yun Sung Lee, Yang Kook Sun, Kee Suk Nahm, Solid State Ionics 118 (1999) 159.
[14] Y. Nitta, K. Okamura, K. Haraguchi, S. Kobayashi, A. Ohta, J. Power Sources 54 (1995) 511.
[15] B. Baanov, J. Bourilkov, M. Maldenov, J. Power Sources 54 (1995) 268.
[16] Y. Nishida, K. Nakane, T. Satoh, J. Power Sources 68 (1997) 561.
[17] H. Arai, S. Okada, Y. Sakurai, J. Yamaki, J. Electrochem. Soc. 144 (1997) 3117.
[18] Y. Gao, M.V. Yakovleva, W.B. Ebner, Electrochem. Solid State Lett. 15 (1998) 117.
[19] Chun-Chieh Chang, N. Scarr, P.N. Kumta, Solid State Ionics 112 (1998) 329.
[20] Ryoji Kanno, Takayuki Shirane, Yukishige Inaba, Yoji Kawamoto, J. Power Sources 68 (1997) 145.
[21] P. Suresh, S. Rodrigues, A.K. Shukla, S.A. Shivashankar, N. Munichandraiah, J. Power Sources 112 (2002) 665.
[22] Y. Nitta, K. Okamura, K. Haraguchi, S. Kobayashi, A. Ohta, J. Power Sources 54 (1995) 511.
[23] M.F. Bent, P. Persson, D.G. Agresti, Comput. Phys. Commun. 1 (1969) 67.
[24] N.N. Greenwood, T.C. Gibb, Mössbauer spectroscopy, Chapman and Hall Ltd., London, 1971, p. 241.
[25] B. Banov, J. Bourilkov, M. Maldenov, J. Power Sources 54 (1995) 268.